SCIENTIFIC REPORTS

OPEN

RRM2B Suppresses Activation of the Oxidative Stress Pathway and is Up-regulated by P53 During Senescence

Mei-Ling Kuo[1], Alexander J. Sy[1], Lijun Xue[1], Martin Chi[1], Michelle T. -C. Lee[1], Terence Yen[1], Mei-Iok Chiang[1], Lufen Chang[1], Peiguo Chu[2] & Yun Yen[1,3]

[1]Department of Molecular Pharmacology, Beckman Research Institute, City of Hope, Duarte, CA 91010, USA, [2]Department of Pathology, City of Hope, Duarte, CA 91010, USA, [3]Taipei Medical University, Taipei 110, Taiwan.

RRM2B is the DNA damage-inducible small subunit of ribonucleotide reductase, the rate-limiting enzyme in *de novo* deoxyribonucleoside triphosphate synthesis. Although RRM2B is implicated in DNA repair and the maintenance of mitochondrial DNA content, the regulation and function of RRM2B in senescence have not been previously established. Here, we show that RRM2B is highly induced in a p53-dependent manner during senescence in primary human fibroblast IMR90 cells and is expressed at higher levels in senescent precancerous human prostatic intraepithelial neoplasm lesions compared to adjacent normal prostate glands. Paradoxically, silencing RRM2B expression leads to an increase in the level of reactive oxygen species, mitochondrial membrane depolarization, and premature senescence in a p38MAPK- and p53-dependent manner in young fibroblasts. Consistently, induction of senescence is accelerated in Rrm2b deficient mouse embryo fibroblasts. Our data demonstrate that RRM2B is induced by stress signals prior to the onset of senescence and prevents premature oxidative stress-induced senescence.

Ribonucleotide reductase (RR) consists of two large subunits, RRM1, and two small subunits, RRM2 or RRM2B (also known as p53R2)[1]. RRM1 expression is constant throughout the cell cycle, whereas that of RRM2 is elevated during the S-phase to boost RR activity[2,3] and is degraded during the G2/M[4] and G1 phases[5]. RRM2B is induced upon activation of the DNA damage pathway transcriptionally by p53[6–8] and post-translationally by ATM[9]. DNA damage-induced RRM2B forms an active complex with RRM1 to supply deoxyribonucleoside triphosphates (dNTPs) for DNA repair[1]. Mutations and deletions in the *RRM2B* locus are associated with human diseases, including mitochondrial DNA (mtDNA) depletion syndrome, suggesting that RRM2B plays an essential role in the maintenance of mitochondrial DNA content[10]. Mice with a germline homozygous *Rrm2b* deletion develop normally and are viable at birth but show growth retardation and early mortality due to severe renal failure[8], highlighting the importance of Rrm2b in physiological function.

The tumor suppressor P53 responds to stress by inducing a repertoire of transcriptional targets that are involved in distinct biological processes, including cell cycle arrest, senescence and apoptosis, depending on the biological setting[11]. Senescence was first characterized in primary human fibroblasts as a state of permanent growth arrest while maintaining active metabolism and can be triggered by various signals, such as telomere shortening, oncogenic stress and DNA damage[12]. It has been demonstrated *in vivo* that senescence is a *bona fide* tumor suppressive mechanism and not just an "artifact" of cell culture[13–16]. Growing evidence indicates that senescence is far more complex than a simply irreversible cessation of cell proliferation. The senescence-associated secretory phenotype not only enforces growth arrest but also promotes tissue repair, immune clearance, aging and tumorigenesis[17].

Given the essential roles of p53 and the DNA damage response in both the induction of senescence and the regulation of RRM2B expression, we hypothesized that RRM2B might be functionally linked to the senescence pathway. Our results provide the first evidence that RRM2B is involved in suppressing the elevation of reactive oxidative species (ROS) levels in physiological conditions as well as those of overt oxidative stress. It is highly up-regulated in response to stress signals in a p53-dependent manner in senescent primary human fibroblasts and human precancerous lesions. Our data suggest that RRM2B is not part of senescence program itself but rather a negative modulator that impedes the activation of oxidative stress signals that prematurely induce senescence.
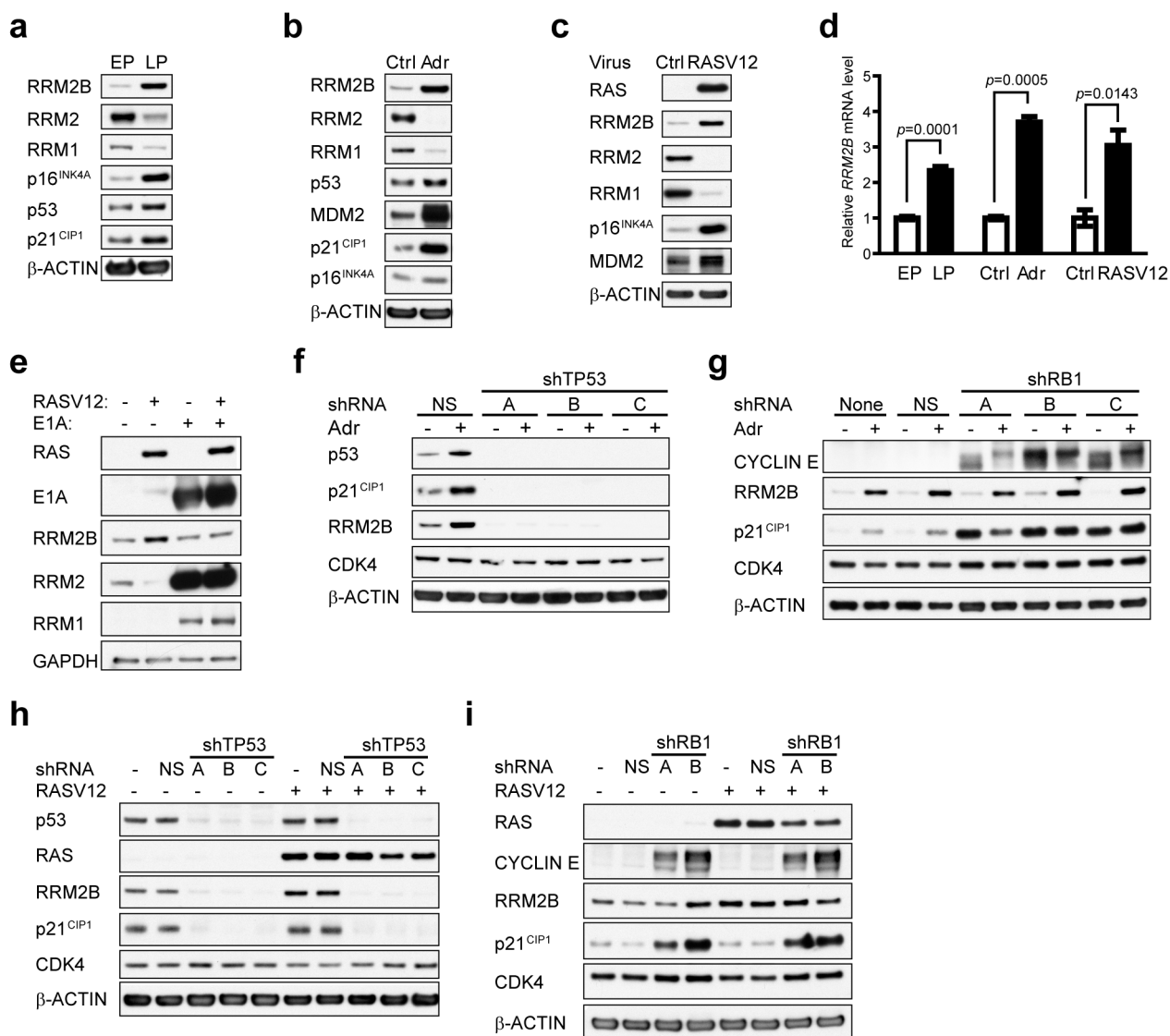
Figure 1 | RRM2B is up-regulated during replicative- and stress-induced senescence in a p53-dependent manner. (a) Western blot analysis of proteins in early passage (EP, ~20–30 PD) and late passage (LP, additional 35 PD) IMR90 cells. (b) Western blot analysis of proteins in IMR90 cells without treatment (Ctrl) or treated with 0.1 μg/ml Adriamycin (Adr) for one week. (c) Western blot analysis of proteins in IMR90 cells expressing either empty vector (Ctrl) or oncogenic RASV12. Cells were harvested 2 weeks following retroviral infection. (d) *RRM2B* mRNA levels from IMR90 cultures as described in (a), (b) and (c) were quantified by real-time RT-PCR. *β-ACTIN* or *GAPDH* were used as internal controls. Relative *RRM2B* mRNA levels from senescent IMR90 cells (■) were normalized to the values from non-senescent controls (□) (means±SEM, *n*=3). (e) Western blot analysis of proteins in IMR90 cells transduced with both MSCV and pLPC retroviruses expressing either vector alone, RASV12, E1A or both RASV12 and E1A. Cells were analyzed two weeks following retroviral infection. (f, g) Western blot analysis of proteins in IMR90 cells expressing pSUPER.retro.puro empty vector, non-silencing shRNA (shNS), shTP53 in (f) or shRB1 in (g) as indicated. One week following infection, cells were treated with 0.1 μg/ml Adriamycin for an additional week prior to analysis. (h, i) Western blot analysis of proteins in IMR90 cells transduced with both MSCV and pSUPER.retro.puro retroviruses expressing empty vector, shRNA, RASV12 or both shRNA and RASV12. The cells were analyzed 2 weeks following infection.

Results

RRM2B is induced during senescence. Although RRM2B was identified as a transcriptional target of p53, its role in the senescence pathway is not well understood. We first examined RRM2B expression in the primary human diploid fibroblast cell strain IMR90, which retains an intact DNA damage response pathway (Supplementary Fig. S1a) and undergoes replicative senescence due to telomere attrition after 50–60 population doublings. Interestingly, the RRM2B protein level was profoundly elevated along with several other senescence regulators, such as p53, p21[CIP1] and p16[INKA12], in late passage (LP) senescent IMR90 cells compared to early passage (EP) IMR90 cells (Fig. 1a, and Supplementary Fig. S2a).

Other stress signals, such as activated oncogenes or DNA damage, can trigger senescence in fibroblasts during early passage, which is defined as "premature senescence"[18]. Similar to cells undergoing replicative senescence, RRM2B expression was also increased in prematurely senescent cells induced by treatment with low-dose Adriamycin or by the expression of oncogenic RASV12 (Fig. 1, b and c and Supplementary Fig. S2, b and c). Unlike RRM2B, both RRM1 and RRM2 levels were reduced upon the induction of senescence (Fig. 1, a, b and c). Furthermore, the *RRM2B* mRNA level was significantly higher in senescent cells compared to untreated young fibroblasts (Fig. 1d), suggesting that the induction of RRM2B is controlled, at least in part, at the transcriptional level.
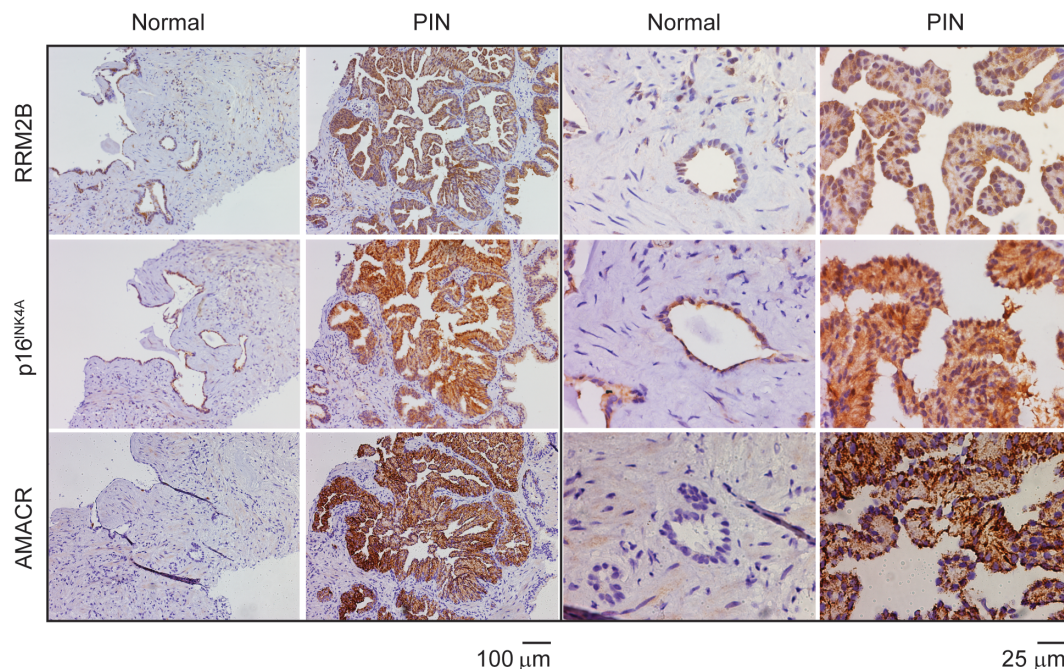
| | Normal | PIN | Normal | PIN |

Figure 2 | RRM2B is highly expressed in precancerous prostate intraepithelial neoplasm (PIN) lesions. Immunocytochemistry staining was performed to detect RRM2B (top), p16[INK4A] (middle) and AMACR (bottom) in prostate tissue sections that contain PIN lesions and in the surrounding normal prostate glands. A representative normal prostate gland and PIN lesion for each staining are matched and shown at low (left) and high magnifications (right).

RRM2B expression was not significantly altered when the proliferation of IMR90 cells was acutely ceased by overexpressing p21[CIP1] (Supplementary Fig. S3), implying that the induction of RRM2B during senescence is controlled by specific pathways and is not simply the consequence of cell cycle arrest during senescence.

The induction of RRM2B depends on p53 in senescent IMR90 cells. Inactivation of both the p53 and RB pathways with the adenovirus oncoprotein E1A overrides RASV12-induced senescence[18,19]. We co-expressed RASV12 and E1A in IMR90 cells and found that E1A abolished the induction of RRM2B by RASV12 (Fig. 1e). This finding further establishes the correlation between RRM2B induction and senescence under stress. To interrogate which of the two most important regulators of the senescent program[20], i.e., p53 and RB, govern RRM2B expression, we expressed short hairpin RNAs (shRNAs) to silence the expression of *TP53* and *RB1*, respectively. Like p21[CIP1], both the basal and Adriamycin-induced expression of RRM2B was significantly curtailed upon the silencing of p53 (Fig. 1f). CDK4 expression was not influenced by p53 knockdown, demonstrating the specificity of the shTP53s (Fig. 1f). In contrast, silencing of RB1, indicated by an increase in CYCLIN E due to the activation of E2F, had no detectable effect on RRM2B in the presence or absence of Adriamycin. The p21[CIP1] expression level was elevated in RB1-silenced cells (Fig. 1g), presumably due to the activation of p53 by the induction of Ser15 phosphorylation[20]. The mode of RRM2B regulation during chronic stress-induced senescence is reminiscent of the response to acute DNA damage in IMR90 cells (Supplementary Fig. S1, b and c). Using an identical approach, we found that the induction of RRM2B by RASV12 was also abolished by the expression of shTP53 but not shRB1 (Fig. 1, h and i). Taken together, p53 tumor suppressor exclusively regulates RRM2B expression in stress-induced senescent cells.

RRM2B is highly expressed in human prostate precancerous lesions. Oncogenic stress-induced senescence in precancerous lesions in murine models and humans has been recently documented[13–16,21–23].

Inactivation of *Pten* in the prostate of mice induces the onset of precancerous high-grade prostatic intraepithelial neoplasia (HG-PIN) and p53-dependent senescence[13]. Loss of *Tp53* in *Pten*-deficient prostates can fully rescue oncogene-induced senescence and convert HG-PIN to invasive prostate cancer[13]. To confirm the correlation between RRM2B and senescence *in vivo*, we performed immunohistochemistry to evaluate the expression of RRM2B and p16[INK4A] in human PIN lesions, which display a senescent phenotype[21], in comparison with adjacent normal prostate glands. PIN lesions typically showed positive staining for alpha-methylacyl-CoA (AMACR) (Fig. 2) and possessed an intact layer of surrounding basal cells that express cytoplasmic, high molecular weight (HMW) KARATIN and nuclear p63[24] (Supplementary Fig. S4). In contrast, AMACR was undetectable in the normal prostate gland (Fig. 2, bottom panel). The expression of both RRM2B and p16[INK4A] in PIN lesions was strikingly higher compared to the surrounding normal prostate glands (Fig. 2). To support our finding, we searched the Oncomine expression array database for a larger sample size and found that the RRM2B mRNA level was 3.8-fold higher in PIN lesions compared to normal prostate glands ($p=3.07E-5$)[25].

Silencing of *RRM2B* triggers premature senescence in young IMR90 cells. We next sought to understand the physiological role of RRM2B in senescence by expressing shRNAs to silence RRM2B in IMR90 cells. RRM2B was efficiently silenced by three shRRM2Bs that target different regions of *RRM2B* mRNA compared to cells expressing scramble non-silencing shRNA (shNS) and an empty vector (Fig. 3a). Because RRM2B was up-regulated during senescence, we postulated that knockdown of RRM2B might impair the induction of senescence. Unexpectedly, the silencing of RRM2B triggered premature senescence (Fig. 3b) in young IMR90 cells. We introduced three point mutations (shRRM2B-mut) within shRRM2B-C (designated as shRRM2B) to interfere with the cleavage of *RRM2B* mRNA. ShRRM2B-mut did not silence endogenous RRM2B (Supplementary Fig. S5) and could no longer induce SA-β-gal activity (Fig. 3d) or suppress DNA replication (Fig. 3e). The
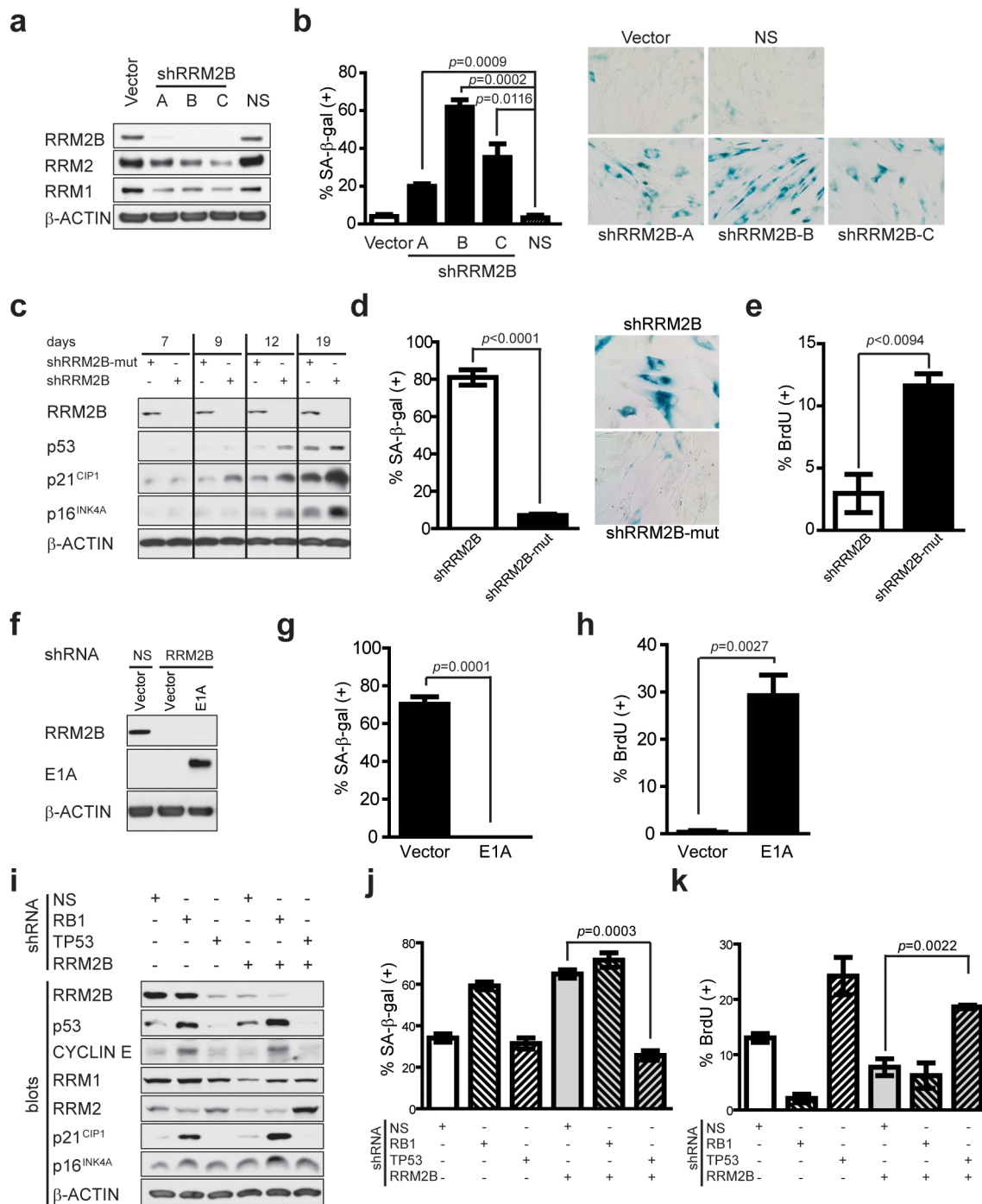
Figure 3 | Silencing of RRM2B induces premature senescence in IMR90 cells. (a) Western blot analysis of proteins in IMR90 cells expressing pSUPER.retro.Puro empty vector, shNS or three different shRRM2Bs. Cells were analyzed two weeks after retroviral infection. (b) Left: senescence associated β-galactosidase (SA-β-gal) activity in cells as described in (a) (means±SEM, $n=3$); right: representative photographs. (c) Western blot analysis of proteins in IMR90 cells expressing shRRM2B-mut or shRRM2B at various time points following retroviral infection. (d) Left: SA-β-gal activity in cells expressing shRRM2B or shRRM2B-mut three weeks following infection (means±SEM, $n=3$); right: representative photographs. (e) A BrdU incorporation assay was performed to analyze cell proliferation 3 weeks following infection (means±SEM, $n=3$). (f) Western blot analysis of proteins in IMR90 cells expressing shRRM2B alone or co-expressing E1A and shRRM2B. Cells expressing shNS and MSCV empty vector were used as a control. Cells were analyzed 2 weeks following retroviral infection. (g) SA-β-gal activity and (h) the BrdU incorporation index in cultures as described in (f) (means±SEM, $n=3$). (i) Western blot analysis of proteins in IMR90 cells expressing shNS, shTP53-A or shRB1-A alone or in combination with shRRM2B. (j) SA-β-gal activity and (k) the BrdU incorporation index in cultures as described in (i) (means±SEM, $n=3$).

specific silencing of RRM2B led to the progressive accumulation of multiple senescent regulators, including p53, p21^{CIP1} and p16^{INK4A}, from day 7 to 19 (Fig. 3c). Furthermore, gene expression profiling by microarray analysis and Gene Ontology (GO) enrichment analysis

demonstrated that genes involved in cell cycle progression, DNA damage repair and DNA metabolism were significantly down-regulated and that genes involved in the immune response were up-regulated in cells expressing shRRM2B compared to those
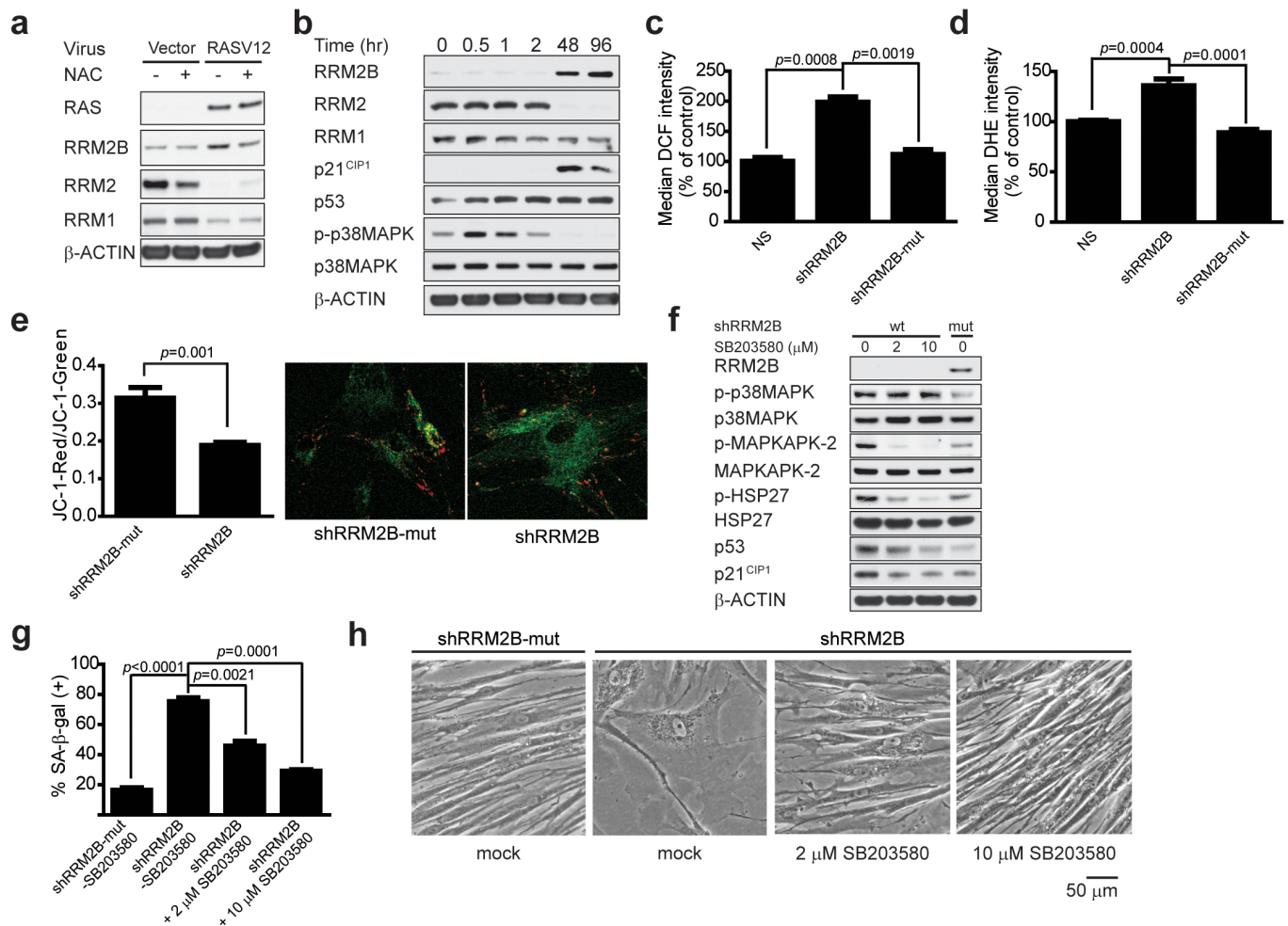
Figure 4 | **RRM2B is induced upon oxidative stress and suppresses the ROS level under normal physiological conditions.** (a) Western blot analysis of proteins in IMR90 cells expressing RASV12 or empty vector. Cells were treated with 2 mM N-acetyl-cysteine (NAC) two days post-infection and harvested after an additional 12 days. (b) Western blot analysis of proteins in IMR90 cells that were treated with 200 µM H_2O_2 for 2 hours and then allowed to incubate for 96 hours. (c) The DCF or (d) DHE fluorescence intensity in IMR90 cells expressing shNS, shRRM2B and shRRM2B-mut was measured by flow cytometry (means±SEM, $n=3$ for DCF and $n=6$ for DHE) to detect multiple ROS, including hydrogen peroxide, the hydroxyl radical, the peroxyl radical, and the peroxynitrite anion by DCF staining and superoxide by DHE staining. (e) JC-1 red and green fluorescence in IMR90 cells expressing either shRRM2B-mut or shRRM2B 2 weeks after retroviral infection were visualized by confocal microscopy. Total green and red fluorescence intensities from randomly selected fields were measured and quantified. JC-1 Red/JC-1 Green ratios are plotted in the left panel (means±SEM, $n=5$). Representative photographs are shown in the right panel. (f) Western blot analysis of proteins in IMR90 cells expressing shRRM2B or shRRM2B-mut and treated with either vehicle (DMSO) or SB203850 for 2 weeks. (g) SA-β-gal activity assays were performed to quantify senescence (means±SEM, $n=3$) in cells as described in (f). (h) Cultures as described in (f) were photographed to show morphology.

expressing shRRM2B-mut (Table S3–6). This expression profile further validates certain senescent phenotypes in *RRM2B*-silenced IMR90 cells.

Induction of premature senescence by silencing *RRM2B* is mediated by p53. Knockdown of RRM2B did not further augment RASV12-induced premature senescence (Supplementary Fig. S6a–c), which is mediated by the activation of both RB and p53[20], suggesting that common downstream pathways were activated by RASV12 and shRRM2B. Consistent with this view, E1A completely rescued shRRM2B-induced premature senescence (Fig. 3, g and h). Interestingly, the silencing of p53 by shRNA in shRRM2B-expressing cells (Fig. 3i) was sufficient to rescue premature senescence, as indicated by the significant reduction in SA-β-gal activity (Fig. 3j) and the increase in the replication index (Fig. 3k). Cells expressing both shRRM2B and shTP53 showed reduced expression of p21[CIP1] and increased levels of RRM1 and RRM2 (Fig. 3i), whereas p16[INK4A] was unchanged (Fig. 3i) compared to

cells expressing shRRM2B alone. In contrast, knockdown of RB1 triggered the activation of the p53 pathway (Fig 3i) and was unable to rescue shRRM2B-triggered premature senescence (Fig. 3, j and k). Taken together, the silencing of RRM2B under normal physiological conditions triggers p53-dependent premature senescence in IMR90 cells.

The expression of RRM2B increases in response to oxidative stress. Senescent human fibroblasts displayed aberrant mitochondrial function and biogenesis as well as an elevated level of reactive oxygen species (ROS)[26–28], which, in part, mediate stress-induced senescence[29]. Hence, it is likely that elevated RRM2B expression during senescence is a response to increased oxidative stress. To test this hypothesis, RASV12-expressing IMR90 cells were treated with N-acetyl cysteine (NAC) to increase the intracellular antioxidant level. Treatment of RASV12-expressing cells with NAC reduced the level of RRM2B, while changes in RRM1 and RRM2 were nearly undetectable (Fig. 4a). To further demonstrate that
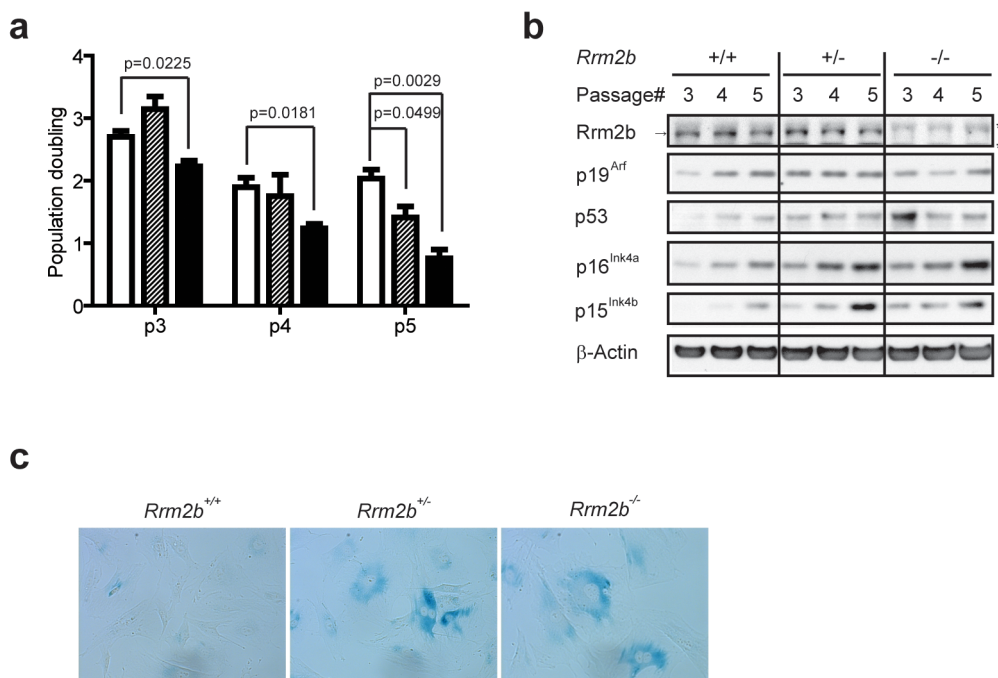
Figure 5 | *Rrm2b*$^{+/-}$ and *Rrm2b*$^{-/-}$ MEFs undergo premature senescence compared to *Rrm2b*$^{+/+}$ MEFs. MEFs derived from different *Rrm2b* genotypes were generated and maintained by a defined 3T3 protocol. (a) Population doubling of MEFs was quantified 3 days after dilution and re-plating from passage 3 to 5 (means±SEM, *n*=3). □: *Rrm2b*$^{+/+}$; ▨: *Rrm2b*$^{+/-}$; ■: *Rrm2b*$^{-/-}$. (b) Western blot analysis of known senescence regulators in MEF strains with different *Rrm2b* genotypes from passage 3 to 5. *: non-specific bands; →: Rrm2b specific band. (c) A SA-β-gal activity assay was performed in MEFs with different *Rrm2b* genotypes at passage 5.

RRM2B expression is related to an increase of oxidative stress, IMR90 cells were transiently treated with 200 μM H_2O_2 for 2 hours and allowed to incubate for up to 96 hours. P38MAPK Thr180/Tyr182 phosphorylation was transiently induced during the H_2O_2 treatment, indicating the onset of the oxidative stress response[30] (Fig. 4b). Unlike p53, which increased immediately, the RRM2B protein level slowly increased, starting at 20 hours (Supplementary Fig. S7a) and reaching a significantly higher level at 48 hours and 96 hours (Fig. 4b), suggesting that additional processes other than p53 accumulation are required for the induction of RRM2B by H_2O_2.

Silencing of *RRM2B* triggers an elevation in ROS and the activation of the p38MAPK pathway. Without overt stress, the cells are continuously exposed to endogenous ROS, which are byproducts of normal respiration. The cellular anti-oxidation system is turned on in response to oxidative stress to prevent damage. Indeed, some of these anti-oxidation proteins are p53 targets[31]. We previously reported that RRM2B shows anti-oxidation activity *in vitro*[32]. Hence, we tested whether the silencing of RRM2B had any effect on antagonizing endogenous ROS *in vivo*. In fact, the ROS level was significantly increased and the mitochondrial membrane was subsequently depolarized in cells expressing shRRM2B compared to cells expressing shNS and shRRM2B-mut (Fig. 4, c, d, and e). Treatment of shRRM2B-expressing IMR90 cells with low dose NAC (0.5 mM) reduced the percentage of β-gal-positive cells from 67.6±3.6% to 52.6±6.3% (*p*=0.005, n=6), suggesting that ROS partly mediates the induction of senescence in RRM2B-silenced cells. We were unable to test the impact of a higher concentration of NAC on the induction of senescence due to a cytostatic effect in IMR90 cells that occurs after long-term exposure to NAC.

It is likely that oxidative stress in RRM2B knockdown cells is derived from impaired mitochondrial function due to reduced mtDNA content. To test this hypothesis, we determined the level of the mitochondrial *COX-1* gene relative to that of the nuclear

β-GLOBIN gene in RRM2B-silenced IMR90 cells compared to non-silenced controls. A slight decrease in the mtDNA content was detected in shRRM2B-expressing cells compared to the control sample (Supplementary Fig. S8), suggesting that the elevation in ROS might be partially due to a loss of mtDNA content.

We further examined the signaling pathway triggered by oxidative stress, such as the phosphorylation and activation of p38MAPK[33], which is also an essential regulator of the stress-induced senescence program[30,34,35]. Intriguingly, p38MAPK phosphorylation was profoundly increased when RRM2B was silenced compared to shRRM2B-mut-expressing cells (Fig. 4f). Downstream targets of p38MAPK were also activated, as indicated by the significant elevation of phosphorylated MAPKAPK-2, a substrate of p38MAPK, and the phosphorylation of HSP27, a substrate of MAPKAPK-2[36] (Fig. 4f). Treatment of RRM2B-deficient cells with the p38MAPK inhibitor SB203580[37] efficiently reduced the level of phosphorylation of both MAPKAPK-2 and HSP27 in a dose-dependent manner and also suppressed the activation of both p53 and p21^{CIP1}. Not only did SB203580 partially reduce SA-β-gal activity (Fig. 4g), it also prevented the morphological change induced by silencing RRM2B, which was typically flat and enlarged compared to non-senescent cells (Fig. 4h).

Conversely, we overexpressed RRM2B in IMR90 cells and tested if RRM2B suppressed ROS levels in response to exogenous oxidants. Overexpression of RRM2B did not affect the basal ROS level in IMR90 cells under normal physiological conditions (Supplementary Fig. S9a), suggesting that the endogenous level of RRM2B was sufficient to suppress ROS. Interestingly, overexpression of RRM2B antagonized the increase in the level of ROS that was triggered by incubation with H_2O_2 (Supplementary Fig. S9a). Consistently, the increased expression of RRM2B had no impact on p38MAPK activity without H_2O_2 treatment but attenuated the activation of the p38MAPK pathway induced by H_2O_2, as indicated by the reduced levels of phospho-p38MAPK and phospho-MAPKAPK-2 (Supplementary Fig. S9b) compared to those in vector-expressing cells treated with H_2O_2.
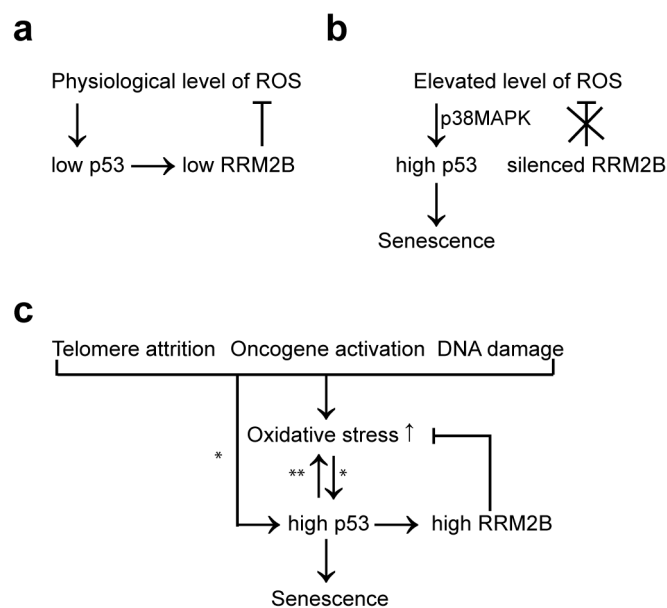
a Physiological level of ROS

low p53 ⟶ low RRM2B

b Elevated level of ROS

p38MAPK

high p53   silenced RRM2B

Senescence

c Telomere attrition Oncogene activation DNA damage

Oxidative stress ↑

* ** *

⟶ high p53 ⟶ high RRM2B

Senescence

Figure 6 | Stochastic models of RRM2B in oxidative stress and senescence pathways in normal primary human fibroblasts. (a) Generation of ROS by cellular metabolic activity induces a low level of p53 and a low level of RRM2B, which keeps ROS at a non-harmful level. (b) Silencing of RRM2B in young primary fibroblasts during early passage disables the negative feedback control and leads to an elevation in ROS. Increased oxidative stress triggers the up-regulation of p53 and ultimately induces senescence. (c) Several stress signals trigger a high level of p53 (*), which transactivates a high level of RRM2B. Although RRM2B is expressed at a high level in stress-induced senescent cells, it does not completely overcome the overt oxidative stress triggered by multiple pathways, including the supraphysiological level of p53 that induces several oxidative genes as positive feedback regulation (**). Hence, the RRM2B level remains high due, at least in part, to persistent oxidative stress.

Our data demonstrate that RRM2B suppresses the ROS level under normal physiological and overt oxidation conditions *in vivo*; however, it is not clear if RRM2B is directly involved in detoxification through its tyrosyl radical or if it indirectly activates another protein to provide the anti-oxidation function. To test the former hypothesis, we treated senescent IMR90 cells that were induced by chronic exposure to low dose Adriamycin or by the expression of oncogenic RASV12 with hydroxyurea (HU) to scavenge the tyrosyl radical and measured the total ROS levels. There was no detectable effect of HU on the ROS level in Adriamycin- or RASV12-induced senescent cells (Supplementary Fig. 10). Our data suggest that the tyrosyl radical in RRM2B does not contribute to the anti-oxidation function of RRM2B, and most likely, RRM2B elicits its anti-oxidation function through the activation of an anti-oxidation protein or the inhibition of an oxidation protein.

The induction of senescence is accelerated in mouse embryo fibroblasts (MEFs) derived from $Rrm2b^{+/-}$ and $Rrm2b^{-/-}$ mice compared to their $Rrm2b^{+/+}$ counterparts. MEFs derived from wild-type mice undergo senescence upon successive transfer using the 3T3 protocol[38]. Both p19[Arf] and p16[Ink4a] are progressively up-regulated to activate the p53 and Rb pathways, respectively, before the onset of senescence[39]. Unlike primary human fibroblasts, in which both the p53 and RB pathways are required to trigger senescence, only the Arf/p53 tumor suppressor pathway is essential to induce and maintain cellular senescence in MEFs[40]. To further support our findings from IMR90 cells, we generated MEFs derived from $Rrm2b^{+/+}$, $Rrm2b^{+/-}$ and $Rrm2b^{-/-}$ mice[41] to test the impact of $Rrm2b$ loss on the induction of senescence. MEF cultures

were maintained *in vitro* on a defined "3T3" schedule. At passage 3–5, wild type MEFs underwent ~2 population doublings in the 3 days prior to dilution and replating. The proliferation of $Rrm2b^{-/-}$ MEFs was significantly retarded, as indicated by the reduction of the population doublings (Fig. 5a). The population doubling rate of $Rrm2b^{+/-}$ MEFs at p3 and p4 was similar to that of $Rrm2b^{+/+}$ MEFs but was significantly reduced at p5. The expression of known senescence regulators was analyzed in MEFs with different $Rrm2b$ genotypes. At passage 3, levels of p19[Arf], p53, p16[Ink4a] and p15[Ink4b] were higher in $Rrm2b^{+/-}$ and $Rrm2b^{-/-}$ MEFs compared to those of $Rrm2b^{+/+}$ MEFs (Fig. 5b). Both p16[Ink4a] and p15[Ink4b] progressively accumulated after two more passages (Fig. 5b). In contrast to wild type MEFs, $Rrm2b^{+/-}$ and $Rrm2b^{-/-}$ MEFs displayed an enlarged and flattened cell morphology and showed a significant elevation in SA-β-gal activity at p5 (Fig. 5c). The SA-β-gal activity continued to increase over the next two passages in $Rrm2b^{+/-}$ and $Rrm2b^{-/-}$ MEFs, while wild type MEFs showed minimal SA-β-gal activity (Supplementary Fig. S11). Furthermore, Rrm2b-deficient MEFs were more sensitive to RASV12-induced premature senescence, as indicated by the elevated levels of senescence regulators and higher SA-β-gal activity compared to wild-type MEFs expressing RASV12 (Supplementary Fig. S12). Consistent with the results from our studies of shRRM2B-expressing IMR90 cells, Rrm2b protects cells from premature senescence during early passage in MEFs.

Discussion

In this report, we demonstrated that under normal physiological conditions, low-level RRM2B suppressed the elevation of endogenous ROS (Fig. 6a). Silencing of RRM2B disabled the negative feedback control and led to increased oxidative stress, which triggered p38MAPK- and p53-dependent senescence (Fig. 6b). Similar to our findings, Sablina et al. previously reported that relative low level of p53 is sufficient to up-regulate several antioxidant genes in the absence of severe stress and that silencing of p53 or its antioxidant target genes under normal physiological conditions leads to an increase in the ROS level[31]. It seems conflicting that p53 activates genes such as RRM2B for anti-oxidation in stress induced-senescent cells, which display an increase in the level of ROS. However, overt oxidative stress induces the p53-dependent up-regulation of multiple pro-oxidation genes in addition to anti-oxidant genes[31]. Hence, the level of ROS is determined by the balance between the actions of "pro-oxidation" and "anti-oxidation" genes, and most likely, the effects of pro-oxidation genes tip the balance to allow for the accumulation of ROS during stress-induced senescence. Ultimately, persistent oxidative stress in normal cells maintains a high level of RRM2B during senescence (Fig. 6c).

Although our data indicate that RRM2B is essential for suppressing ROS levels under normal physiological conditions and that overexpression of RRM2B antagonizes the increase of oxidative stress in response to exogenous oxidants, the molecular mechanism underlying these functions is unknown. There are a few likely scenarios. First, the establishment of senescence requires a dynamic feedback loop between the DNA damage response and ROS production in primary human fibroblasts[27]. Given that RRM2B has an enzymatic function to provide sufficient dNTP pools for DNA damage repair, the accumulation of DNA damage due to poor DNA repair might activate downstream pathways to trigger mitochondrial dysfunction and an elevation in ROS in *RRM2B*-silenced IMR90 cells. Supporting this hypothesis, Arakawa's group previously reported that mouse embryo fibroblasts (MEFs) derived from $Rrm2b^{-/-}$ mice are significantly more sensitive to oxidative stress-induced cell death compared to those derived from wild-type mice[8]. They further demonstrated that impaired Rrm2b function leads to a decrease in dNTP pools and the efficiency of DNA repair in response to oxidative stress and hypothesized that the observed hypersensitivity to hydrogen peroxide is due to the accumulation of DNA damage and an increase

in the mutation rate. However, the impact of Rrm2b deficiency on the ROS level was not analyzed in $Rrm2b^{-/-}$ MEFs. Secondly, RRM2B is implicated in mtDNA replication through the production of dNTP apart from its role in DNA damage repair[42]. Deficiency of RRM2B activity in cells derived from patients with mtDNA depletion syndrome results in low mtDNA content and reduced respiratory chain activities in mitochondria[10]. Mitochondrial dysfunction due to a lack of RRM2B activity might lead to an elevation in the ROS level that is independent of the DNA damage response. In fact, a slight decrease (~20%) in the mtDNA content was detected in RRM2B knockdown IMR90 cells compared to control cells. Although it likely contributes to the elevation in ROS, whether the minimal loss of mtDNA content is the sole mechanism underlying the increase of oxidative stress is unclear. Lastly, RRM2B might be involved in cellular redox homeostasis. The expression of RRM1 and RRM2 during stress-induced senescence was greatly reduced whereas that of RRM2B was significantly elevated, suggesting that RRM2B might have a function that is independent of ribonucleotide reduction. We previously reported that recombinant RRM2B has an intrinsic catalase activity to scavenge H_2O_2[32]. However, whether RRM2B is involved in the detoxification of H_2O_2 in vivo has not been tested. Our current study suggests that the tyrosyl radical of RRM2B is not involved in the detoxification of ROS. Hence, RRM2B might activate or inhibit another protein to provide the anti-oxidation function. Identification of RRM2B binding partners that have functions in pro-oxidation or anti-oxidation will be one approach to demonstrate a more direct role for RRM2B in ROS production.

It remains to be investigated whether the sole function of induced RRM2B is to suppress the observed elevation in ROS during senescence. Apart from RRM1, RRM2B also forms complexes with proteins involved in the DNA damage response, such as ATM[9], the MRE11-RAD50-NBS1 complex[9], ATRIP[9], p53[43] and p21[CIP144]. The activation of a persistent DNA damage response is associated with the induction of senescence[12]. It is plausible that the expression of RRM2B during stress-induced senescence can modulate certain senescence phenotypes via interaction with these factors.

Taken together, our data suggest that RRM2B not only is a senescence marker but plays a critical role in preventing the oxidation of essential cellular molecules. The loss of RRM2B function likely leads to ROS-induced genomic instability, which may contribute to the onset of cancer as well as senescence-triggered pathological conditions.

Methods

Plasmids. The pSUPER.retro.puro or pSUPER.retro.neo+gfp retroviral vectors (OligoEngine, Seattle, WA, USA) were used to express shRNA. The inserted oligonucleotide sequences are listed in Supplementary Table S1. The pBABEpuro-H-RASV12, pLPC and pLPC-12s E1A vectors were obtained from Dr. Scott Lowe (Memorial Sloan-Kettering Cancer Center, NY, USA). H-RASV12 cDNA was subcloned from pBABEpuro into pMSCVhyg (Clontech, Mountain View, CA, USA).

Cell culture and chemicals. Human embryonic lung fibroblasts, IMR90 cells, were purchased from the American Type Culture Collection (Manassas, VA, USA). IMR90 cells and 293T cells were cultured in Dulbecco's Modification of Eagle's Medium (DMEM) (Mediatech, Inc., Manassas, VA, USA) supplemented with 10% fetal bovine serum (FBS) (Omega Scientific, Inc., Tarzana, CA, USA) and penicillin and streptomycin (Invitrogen, Carlsbad, CA, USA). MEFs were derived from 13.5-day-old embryos of $Rrm2b^{+/+}$, $Rrm2b^{+/-}$ and $Rrm2b^{-/-}$ mice[41] as described by Kamijo et al.[40]. MEFs were maintained using a 3T3 protocol from Todaro and Green[38]; 3×10^5 cells were plated in 60-mm diameter dishes in DMEM containing 10% FBS, 2 mM glutamine (Invitrogen), 0.1 mM MEM nonessential amino acids (Invitrogen), 55 µM β-mercaptoethanol (Invitrogen), and 10 µg/ml gentamycin (Invitrogen) and passaged every 3 days. All cells were incubated at 37°C and 5% CO_2 in a humidified incubator. Adriamycin was obtained from the City of Hope Pharmacy (Duarte, CA, USA). EZSolution™ SB 203580 was purchased from BioVision Research Products (Mountain View, CA, USA). N-acetyl-cysteine (NAC) was purchased from Sigma-Aldrich (St. Louis, MO, USA).

Retroviral production and infection. Retroviruses were generated as previously described[45]. IMR90 cells were first infected with the VSV-G pseudotyped retrovirus pWZL-Neo-EcoR that expressed the ecotropic receptor and then selected with 400

µg/ml G418. The derived cells were transduced with ecotropic retroviruses expressing cDNA or shRNAs and selected with 2 µg/ml puromycin (Sigma-Aldrich) or 100 µg/ml hygromycin (EMD Chemicals, Gibbstown, NJ, USA) prior to all assays.

Senescence associated-β-galactosidase (SA-β-gal) activity assay. Cells were fixed with 2% formaldehyde and 0.2% glutaraldehyde in PBS for 5 minutes and washed with PBS twice before staining with a 1 mg/ml 5-bromo-4-chloro-3-indolyl-B-D-galactoside (Research Products International Corp., Mount Prospect, IL, USA) solution that contained 5 mM $K_4[Fe(CN)_6]$, 5 mM $K_3[Fe(CN)_6]$, 150 mM NaCl, 2 mM $MgCl_2$, 7 mM $C_6H_8O_7$ and 25 mM Na_2HPO_4, pH 6.0 overnight at 37°C. Blue staining was visualized by light microscopy and photographed. A total of at least 100 cells were scored from each sample.

Bromodeoxyuridine (BrdU) incorporation assay. Cells were fixed in methanol-acetone (1 : 1 [vol/vol]) 24 h after the addition of BrdU (10 µM), treated for 10 min with 1.5 N HCl, and stained for 1 h with a BrdU antibody (IIB5, Santa Cruz Biotechnology, Santa Cruz, CA, USA) followed by anti-mouse AlexaFluor-594 (Invitrogen). DNA was visualized with 4′-6-diamidino-2-phenylindole (DAPI) (Sigma-Aldrich). A total of at least 100 cells were scored from each sample.

Antibodies and protein detection. We raised rabbit antibodies to a synthetic RRM2B peptide (acetyl-PERPEAAGLDQDERSC-amide; amino acids 4–18) conjugated to keyhole limpet hemocyanin, and the anti-sera were purified by immunoaffinity chromatography using the synthetic RRM2B peptide coupled to agarose beads (custom-made by Rockland Immunochemicals, Gilbertsville, PA, USA). Proteins were detected using primary antibodies against human RRM2B (as described above), mouse Rrm2b (ProSci Incorporated, Poway, CA, USA), RRM1 (United States Biological, Swampscott, MA, USA), RRM2, mouse p15[Ink4b], human p16[INK4A], mouse p16[Ink4a], p19[Arf], p21[CIP1], H-RAS, E1A, GAPDH, CDK4, CYCLIN E (Santa Cruz Biotechnology, Santa Cruz, CA, USA), human p53 (EMD Chemicals, Gibbstown, NJ, USA), mouse p53 (Leica Microsystems Inc, Buffalo Grove, IL, USA), MDM2 (mouse monoclonal antibody clone 2A10, provided by Dr. Arnold Levine), β-ACTIN (Sigma-Aldrich), phospho-p38 MAPK (Thr180/Tyr182), p38MAPK, phosphor-MAPKAPK-2 (T222), MAPKAPK-2, phospho-HSP27(Ser82) and HSP27 (Cell Signaling Technology, Inc., Danvers, MA, USA) using a previously described procedure[45].

Measurement of reactive oxygen species. Cells were harvested by trypsinization, resuspended in PBS containing 2.5 µM CM-H_2DCFDA (Invitrogen) and incubated at 37°C for 30 minutes. Cells were collected by centrifugation, washed twice with PBS and analyzed by flow cytometry. To measure the total superoxide level, cells were collected as described above and stained with 2.5 µM DHE (Invitrogen) in PBS containing 5 mM sodium pyruvate at 37°C for 40 minutes. The samples were then immediately chilled on ice and centrifuged. Cell pellets were washed with ice-cold PBS three times before analysis by flow cytometry.

JC-1 staining and analysis. Cells were incubated with 0.77 µM JC-1 (Invitrogen) for 20 minutes at 37°C and washed twice with Hank's balanced salt solution (Invitrogen). Images were captured using confocal microscopy (Zeiss, LSM510) (Carl Zeiss MicroImaging, LLC, Thornwood, NY, USA). The total green- and red-JC-1 intensities of each sample from five randomly selected fields were analyzed by Zeiss LSM AIM4.2 software (Carl Zeiss MicroImaging, LLC).

Quantitative real time polymerase chain reaction (qRT-PCR). Total RNA was isolated using TRIzol® reagent (Invitrogen), and cDNA was generated according to the manufacturer's instructions (Invitrogen). qRT-PCR was performed in the ABI Prism 7900 HT Sequence Detection System (Life Technologies Corporation, Carlsbad, CA, USA) in a 20-µl mix containing cDNA synthesized from 33 ng of total RNA, 5 µM of each primer and ABI SYBR Green PCR Master Mix (Life Technologies Corporation). Relative gene expression was calculated with the $\Delta\Delta C_t$ method using glyceraldehyde 3-phosphate dehydrogenase (GAPDH) or β-ACTIN as an internal control. Primer sequences are listed in Table S2.

Statistical analysis. We performed Student's t tests with two-tailed distribution and two-sample equal variance in Excel (Microsoft, Redmond, WA, USA).

Immunohistochemistry staining. Five-micrometer-thick sections were prepared from formalin-fixed, paraffin-embedded tissue and deparaffinized in xylene followed by 100% ethanol. The samples were then quenched in 3% hydrogen peroxide, pretreated to promote antigen retrieval by steam in DIVA buffer (Biocare Medical, Concord, CA, USA) for 20 minutes and incubated in Protein Block (Dako Corporation, Carpinteria, CA, USA) for 5 minutes. The slides were incubated with a primary antibody against RRM2B (custom-made by Rockland Immunochemicals), p16[INK4A] (BD Biosciences), AMACR (Dako corporation), HMW KARATIN (Dako corporation) or p63 (Zeta Corporation, Sierra Madre, CA, USA) for 1 hour at room temperature. The slides were washed in Dako Buffer and incubated with the appropriate HRP-labeled secondary antibody (Dako corporation) for 30 minutes. After washing in Dako buffer, the slides were incubated with the chromogen diaminobenzidine tetrahydrochloride (DAB), counterstained with hematoxylin, and mounted.

1. Guittet, O. et al. Mammalian p53R2 protein forms an active ribonucleotide reductase in vitro with the R1 protein, which is expressed both in resting cells in

response to DNA damage and in proliferating cells. *J. Biol. Chem.* **276**, 40647–40651 (2001).

2. Engstrom, Y. *et al.* Cell cycle-dependent expression of mammalian ribonucleotide reductase. Differential regulation of the two subunits. *J. Biol. Chem.* **260**, 9114–9116 (1985).

3. Eriksson, S., Graslund, A., Skog, S., Thelander, L. & Tribukait, B. Cell cycle-dependent regulation of mammalian ribonucleotide reductase. The S phase-correlated increase in subunit M2 is regulated by de novo protein synthesis. *J. Biol. Chem.* **259**, 11695–11700 (1984).

4. D'Angiolella, V. *et al.* Cyclin F-Mediated Degradation of Ribonucleotide Reductase M2 Controls Genome Integrity and DNA Repair. *Cell* **149**, 1023–1034 (2012).

5. Chabes, A. L., Pfleger, C. M., Kirschner, M. W. & Thelander, L. Mouse ribonucleotide reductase R2 protein: a new target for anaphase-promoting complex-Cdh1-mediated proteolysis. *Proc. Natl. Acad. Sci. U. S. A.* **100**, 3925–3929 (2003).

6. Nakano, K., Balint, E., Ashcroft, M. & Vousden, K. H. A ribonucleotide reductase gene is a transcriptional target of p53 and p73. *Oncogene* **19**, 4283–4289 (2000).

7. Tanaka, H. *et al.* A ribonucleotide reductase gene involved in a p53-dependent cell-cycle checkpoint for DNA damage. *Nature* **404**, 42–49 (2000).

8. Kimura, T. *et al.* Impaired function of p53R2 in Rrm2b-null mice causes severe renal failure through attenuation of dNTP pools. *Nat. Genet.* **34**, 440–445 (2003).

9. Chang, L. *et al.* ATM-mediated serine 72 phosphorylation stabilizes ribonucleotide reductase small subunit p53R2 protein against MDM2 to DNA damage. *Proc. Natl. Acad. Sci. U. S. A.* **105**, 18519–18524 (2008).

10. Bourdon, A. *et al.* Mutation of RRM2B, encoding p53-controlled ribonucleotide reductase (p53R2), causes severe mitochondrial DNA depletion. *Nat. Genet.* **39**, 776–780 (2007).

11. Vousden, K. H. & Lane, D. P. p53 in health and disease. *Nat. Rev. Mol. Cell Biol.* **8**, 275–283 (2007).

12. Kuilman, T., Michaloglou, C., Mooi, W. J. & Peeper, D. S. The essence of senescence. *Genes Dev.* **24**, 2463–2479 (2010).

13. Chen, Z. *et al.* Crucial role of p53-dependent cellular senescence in suppression of Pten-deficient tumorigenesis. *Nature* **436**, 725–730 (2005).

14. Collado, M. *et al.* Tumour biology: senescence in premalignant tumours. *Nature* **436**, 642 (2005).

15. Michaloglou, C. *et al.* BRAFE600-associated senescence-like cell cycle arrest of human naevi. *Nature* **436**, 720–724 (2005).

16. Braig, M. *et al.* Oncogene-induced senescence as an initial barrier in lymphoma development. *Nature* **436**, 660–665 (2005).

17. Rodier, F. & Campisi, J. Four faces of cellular senescence. *J. Cell Biol.* **192**, 547–556.

18. Serrano, M., Lin, A. W., McCurrach, M. E., Beach, D. & Lowe, S. W. Oncogenic ras provokes premature cell senescence associated with accumulation of p53 and p16INK4a. *Cell* **88**, 593–602 (1997).

19. Ruley, H. E. Adenovirus early region 1A enables viral and cellular transforming genes to transform primary cells in culture. *Nature* **304**, 602–606 (1983).

20. Chicas, A. *et al.* Dissecting the unique role of the retinoblastoma tumor suppressor during cellular senescence. *Cancer Cell* **17**, 376–387.

21. Acosta, J. C. *et al.* Chemokine signaling via the CXCR2 receptor reinforces senescence. *Cell* **133**, 1006–1018 (2008).

22. Kuilman, T. *et al.* Oncogene-induced senescence relayed by an interleukin-dependent inflammatory network. *Cell* **133**, 1019–1031 (2008).

23. Collado, M. & Serrano, M. Senescence in tumours: evidence from mice and humans. *Nat. Rev. Cancer* **10**, 51–57.

24. Zynger, D. L. & Yang, X. High-grade prostatic intraepithelial neoplasia of the prostate: the precursor lesion of prostate cancer. *Int. J. Clin. Exp. Pathol.* **2**, 327–338 (2009).

25. Tomlins, S. A. *et al.* Integrative molecular concept modeling of prostate cancer progression. *Nat. Genet.* **39**, 41–51 (2007).

26. Moiseeva, O., Bourdeau, V., Roux, A., Deschenes-Simard, X. & Ferbeyre, G. Mitochondrial dysfunction contributes to oncogene-induced senescence. *Mol. Cell. Biol.* **29**, 4495–4507 (2009).

27. Passos, J. F. *et al.* Feedback between p21 and reactive oxygen production is necessary for cell senescence. *Mol. Syst. Biol.* **6**, 347 (2010).

28. Passos, J. F. *et al.* Mitochondrial dysfunction accounts for the stochastic heterogeneity in telomere-dependent senescence. *PLoS Biol.* **5**, e110 (2007).

29. Lee, A. C. *et al.* Ras proteins induce senescence by altering the intracellular levels of reactive oxygen species. *J Biol. Chem.* **274**, 7936–7940 (1999).

30. Zdanov, S., Debacq-Chainiaux, F., Remacle, J. & Toussaint, O. Identification of p38MAPK-dependent genes with changed transcript abundance in H2O2-induced premature senescence of IMR-90 hTERT human fibroblasts. *FEBS Lett.* **580**, 6455–6463 (2006).

31. Sablina, A. A. *et al.* The antioxidant function of the p53 tumor suppressor. *Nat. Med.* **11**, 1306–1313 (2005).

32. Liu, X., Xue, L. & Yen, Y. Redox property of ribonucleotide reductase small subunit M2 and p53R2. *Methods Mol. Biol.* **477**, 195–206 (2008).

33. Frippiat, C., Dewelle, J., Remacle, J. & Toussaint, O. Signal transduction in H2O2-induced senescence-like phenotype in human diploid fibroblasts. *Free Radic. Biol. Med.* **33**, 1334–1346 (2002).

34. Freund, A., Patil, C. K. & Campisi, J. p38MAPK is a novel DNA damage response-independent regulator of the senescence-associated secretory phenotype. *Embo J.* **30**, 1536–1548 (2011).

35. Wang, W. *et al.* Sequential activation of the MEK-extracellular signal-regulated kinase and MKK3/6-p38 mitogen-activated protein kinase pathways mediates oncogenic ras-induced premature senescence. *Mol. Cell. Biol.* **22**, 3389–3403 (2002).

36. Cuenda, A. *et al.* SB 203580 is a specific inhibitor of a MAP kinase homologue which is stimulated by cellular stresses and interleukin-1. *FEBS Lett.* **364**, 229–233 (1995).

37. Kumar, S., Jiang, M. S., Adams, J. L. & Lee, J. C. Pyridinylimidazole compound SB 203580 inhibits the activity but not the activation of p38 mitogen-activated protein kinase. *Biochem. Biophys. Res. Commun.* **263**, 825–831 (1999).

38. Todaro, G. J. & Green, H. Quantitative studies of the growth of mouse embryo cells in culture and their development into established lines. *J. Cell Biol.* **17**, 299–313 (1963).

39. Zindy, F. *et al.* Myc signaling via the ARF tumor suppressor regulates p53-dependent apoptosis and immortalization. *Genes Dev.* **12**, 2424–2433 (1998).

40. Kamijo, T. *et al.* Tumor suppression at the mouse INK4a locus mediated by the alternative reading frame product p19ARF. *Cell* **91**, 649–659 (1997).

41. Powell, D. R. *et al.* Rapid development of glomerular injury and renal failure in mice lacking p53R2. *Pediatr. Nephrol.* **20**, 432–440 (2005).

42. Thelander, L. Ribonucleotide reductase and mitochondrial DNA synthesis. *Nat. Genet.* **39**, 703–704 (2007).

43. Xue, L. *et al.* Wild-type p53 regulates human ribonucleotide reductase by protein-protein interaction with p53R2 as well as hRRM2 subunits. *Cancer Res.* **63**, 980–986 (2003).

44. Xue, L. *et al.* Ribonucleotide reductase small subunit p53R2 facilitates p21 induction of G1 arrest under UV irradiation. *Cancer Res.* **67**, 16–21 (2007).

45. Kuo, M. L., den Besten, W., Thomas, M. C. & Sherr, C. J. Arf-induced turnover of the nucleolar nucleophosmin-associated SUMO-2/3 protease Senp3. *Cell Cycle* **7**, 3378–3387 (2008).

Acknowledgements

Author contributions

M.-L.K. designed and performed the experiments, analyzed and interpreted the data and wrote the paper; A.J.S., L.X., M.C., M.T.-C.L., T.Y., and M.-I.C. performed experiments; L.C. generated the *Rrm2b*^+/+^, *Rrm2b*^+/−^ and *Rrm2b*^−/−^ MEFs; P.C. provided the prostatic intraepithelial neoplasm tissue samples for IHC staining; and Y.Y. supervised the project and wrote the paper.

Additional information

How to cite this article: Kuo, M.-L. *et al.* RRM2B Suppresses Activation of the Oxidative Stress Pathway and is Up-regulated by P53 During Senescence. *Sci. Rep.* **2**, 822; DOI:10.1038/srep00822 (2012).